Title	Technical solutions for automotive intermodulation radar for detecting vulnerable road users
Author(s)	Viikari, Ville; Kantanen, Mikko; Varpula, Timo; Lamminen, Antti; Alastalo, Ari; Mattila, Tomi; Seppä, Heikki; Pursula, Pekka; Saebboe, J.; Shi Cheng; Al-Nuaimi, M.; Hallbjorner,P.; Rydberg, A.
Citation	2009 IEEE 69th Vehicular Technology Conference. Barcelona, Spain, 26-29 April 2009, 5 p.
Date	2009
URL	http://dx.doi.org/10.1109/VETECS.2009.5073875
Rights	Copyright © [2009] IEEE. Reprinted from 2009 IEEE 69th Vehicular Technology Conference. Barcelona, Spain, 26-29 April 2009.

Technical Solutions for Automotive Intermodulation Radar for Detecting Vulnerable Road Users

Ville Viikari, Mikko Kantanen, Timo Varpula, Antti Lamminen, Ari Alastalo, Tomi Mattila, Heikki Seppä and Pekka Pursula
Sensing and Wireless Devices
VTT Technical Research Centre
Espoo, Finland
Firstname.Lastname@vtt.fi

Jone Saebboe
TRIAD as
Lilleström, Norway
Jone.Saebboe@triad.no

Shi Cheng, Mustafa Al-Nuaimi, Paul Hallbjörner and Anders Rydberg
Signals and Systems
Uppsala University
Uppsala, Sweden
Shi.Cheng@angstrom.uu.se,
Paul.Hallbjorner@sp.se

***Abstract*—This paper presents building blocks for a proposed automotive intermodulation radar for detecting and identifying vulnerable road users (VRUs). The intermodulation radar transmits at two frequencies and it has receivers both for normal reflections and for reflections from VRUs at the intermodulation frequency. A possible radar architecture is presented and modulation techniques are discussed. Different mixing elements of radar reflectors are studied with simulations. An antenna structure enabling a wearable reflector that can be integrated into clothes is designed and characterized. The simulated and measured performance of the radar reflector is used to estimate the achievable detection range.**

Keywords-harmonic radar; road vehicle radar; transponders; wearable antennas

I. INTRODUCTION

Vulnerable road users (VRUs), such as pedestrians, bicyclists and motorcyclists have a high risk to be seriously injured in road accidents. Therefore, despite of their relatively low involvement in all road accidents, a large proportion of all fatalities are VRUs. For example, pedestrians, bicyclists, mopedists and motorcyclists counted 42.5 % of all fatalities in road accidents in Europe in 2005 [1].

Automotive radars are becoming standard equipment in premium cars. Commercially available radars are either for blind spot detection (BSD) or for automatic cruise control (ACC). BSD systems ease certain maneuvering, such as lane changing, whereas ACC systems adjust the vehicle speed according to the preceding vehicle. In addition to these purposes, multipurpose radar sensors could also be used to detect road conditions [2] or identify VRUs.

One possibility to identify VRUs with automotive radar is to add a harmonic receiver to automotive radar and to equip VRUs with mixing radar reflectors producing backscattering at harmonic frequencies. A harmonic radar, first suggested for vehicle detection by Staras and Shefer [3], detects active or passive transponders (called also reflectors or tags) that when irradiated with a certain frequency, emits a harmonic frequency. This harmonic frequency is offset from the transmitted frequency and all other reflections. Therefore the reflections from tags can be easily separated from the reflections from other objects. Harmonic radar concept is successfully used for example for tracking insects [4]–[6]. However, the frequency regulations set for automotive radars can not be met due to large frequency offset of the harmonic radar. We propose intermodulation radar for detecting and identifying VRUs. As compared to harmonic radar, this concept enables smaller frequency offset easing to fulfill the frequency regulations and facilitating the circuit design.

This paper is organized as follows: Section II presents the intermodulation radar, Section III discusses wearable radar reflectors, their potential mixing elements and antennas, Section IV estimates the achievable detection range and Section V concludes the paper.

II. INTERMODULATION RADAR

The proposed intermodulation radar transmits at two frequencies f_1 and f_2, see Fig. 1. VRUs are equipped with mixing radar reflectors that when illuminated at two frequencies produces their intermodulation frequencies, such as $2f_1 - f_2$. Contrary to mixing radar reflectors, normal targets such as cars, reflects only at the fundamental frequencies f_1 and f_2. Therefore, the intermodulation radar is able to distinguish between two types of the targets due to the frequency offset of the reflected signals.

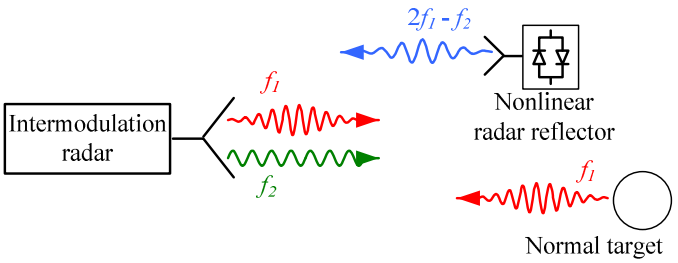

Figure 1. The intermodulation radar transmits signals at two frequencies. Normal targets reflect at the fundamental frequencies whereas nonlinear radar reflectors reflect at an intermodulation frequency.

This work was supported in part by the EU Commission under the contract FP7-ICT-2007-1-216049 of the ADOSE project

A. Frequency Allocation

Currently two frequency bands are allocated for automotive radars in Europe, 22–24 GHz temporary band for short range (30 m) radars [7] and 76–77 GHz band for long range (150 m) radars [8]. The third band, 77–81 GHz, is being currently allocated by European Telecommunications Standards Institute (ETSI) for short range (30 m) automotive radars [9]. We focus on the 76–77 GHz band, even though the intermodulation radar could be realized at the other bands as well.

B. Modulation

The radial resolution of the radar depends on the bandwidth, and it is given as (a rule-of-thumb) $\Delta r = c/(2BW)$, where c is the speed of light and BW is the bandwidth. For example, 0.25 m radial resolution requires a bandwidth of 600 MHz. In addition to the intermodulation radar unit, the radar reflectors must also satisfy the bandwidth requirement.

Several different waveforms (or modulation techniques) can be used with intermodulation radar to generate a transponder return of sufficient bandwidth in a typical FMCW or LFM system [10]. Four examples are briefly discussed in the following and the corresponding frequency-time dependencies of different signals are displayed in Fig. 2.

A) f_1 and f_2 are swept at the same rate whereas the sweeping rate of the intermodulation signal is also the same.

B) f_1 and f_2 are swept at different rates and the intermodulated signal sweeps at mean rate.

C) f_1 is swept and f_2 kept constant, whereas the intermodulated signal sweeps at double rate.

D) f_1 and f_2 are hopped in frequency for improving the interference rejection.

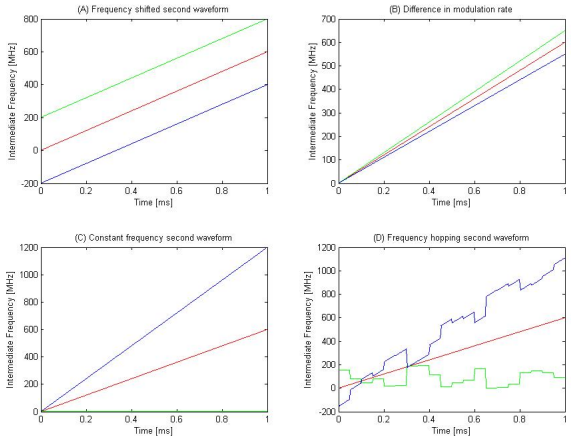

Figure 2. Possible waveforms with intermodulation radar (in the intermediate frequency band). f_1 is in red, f_2 is in green and the reflected intermodulation signal at $2f_1-f_2$ is in blue.

Each of these waveforms can be realized either in separate bands or in one band. For separate bands, the frequency difference between f_1 and f_2 is greater than twice the channel BW of the receiver. In this case the radar receiver has two non-overlapping channels at $2f_1 - f_2$ and at f_1. This method would result in a higher dynamic range. In addition, the intermodulated signal at $2f_1 - f_2$ would not be mixed with Doppler shifted reflections from conventional targets at f_1. The channel BW could be rather narrow. However, two receiver channels that are separated in frequency would be required for the radar system.

If the frequency difference between f_1 and f_2 is small, the intermodulation signal and the base signal at f_1 are in the same channel. In this case the intermodulation frequency mixes with the Doppler shifted signal at f_1 resulting in in-band intermodulation products of the two base frequencies degrading the dynamic range of the system. However, system wise this method gives a minimum of hardware modifications to conventional automotive radar.

C. Prototype Radar System

The first automotive intermodulation radar is under development. The monostatic design is based on voltage controlled oscillators under computer control. A complete transceiver subsystem for f_1 enables operation as conventional automotive radar whereas other subsystems transmit at f_2 and receives the intermodulation signal at $2f_1 - f_2$.

III. Wearable Radar Reflectors

Our objective is to design relatively small and low-cost radar reflectors that can be integrated into clothing. In order to keep manufacturing costs low, the reflectors are not allowed to contain a battery. The structure of the radar reflectors is similar to those used for insect tracking [4] – [6]: a mixing element, such as a diode, is matched directly to the antenna. Other possible mixing elements in addition to a diode are ferroelectric varactor and MEMS resonator.

The mixing elements should be able to mix at extremely low power levels from –15 dBm to –35 dBm (typical mixers require at least 0 dBm). In the following, we study by harmonic-balance simulation, which mixing element, Schottky diode, ferroelectric varactor or MEMS resonator offers the lowest mixing loss at these low power levels. The mixing elements are matched to a 50 Ω source (antenna) with optimized three-degree microstrip matching circuits.

A. Schottky-Diode as a Mixing Element

The Schottky diode is the most commonly used nonlinear element in mm- and submm-wave frequency multipliers [11] and mixers [12]. Two Schottky diodes available as MMIC chips were selected as test diodes for simulations. The first diode is DBES105a from United Monolithic Semiconductors[1] S.A.S. (UMS), France, and the other is G2APD32fG111 from Virginia Diodes[2], Inc. (VDI), USA. Both chips contain two identical diodes in antiparallel configuration, which makes the capacitance-voltage dependence symmetric at zero bias maximizing the third order mixing efficiency. The parameters of the diodes are shown in Table I and the simulated conversion losses in Fig. 3.

[1] http://www.ums-gaas.com
[2] http://www.virginiadiodes.com

TABLE I. THE PARAMETERS OF SIMULATED SCHOTTKY DIODES.

	UMS	VDI
Saturation current (A)	1.6e-13	1.1e-14
Series resistance (Ω)	2.8	3.0
Ideality factor	1.28	1.13
Zero-bias junction capacitance (fF)	3.4	15.0
Built-in voltage (V)	0.55	0.52
Parasitic capacitance (fF)	25.5	23.5

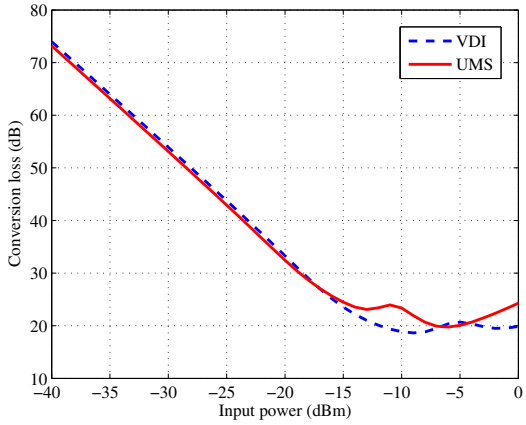

Figure 3. The simulated conversion losses of the Schottky diodes.

The diodes have approximately equal performance. The mixing loss is inversely proportional to the square of the input power at low power levels (< –15 dBm).

B. *Ferroelectric Varactor as a Mixing Element*

The relative permittivity of ferroelectric materials tends to be high (from hundreds to thousands) and it depends on the external electric field. Typical ferroelectric materials are Barium Titanate and Barium Strontium Titanate [13].

These materials can be used in several microwave components, such as varactors [14]. The voltage dependence of Barium Strontium Titanate varactor can be expressed as [15]

$$C_{fe}(V) = \frac{C_{max}}{2\cosh\left[\frac{2}{3}\sinh^{-1}\left(\frac{2V}{V_{1/2}}\right)\right]-1}, \qquad (1)$$

where C_{max} is the maximum capacitance (depends on the geometry and the relative permittivity of ferroelectric film) and $V_{1/2}$ is the voltage at which the capacitance is halved of its maximum value. The voltage dependence of the capacitance is symmetric and it is therefore ideal for producing third order mixing products at zero bias.

We have simulated two different Barium Strontium Titanate varactors having equal mechanical dimensions, but different Barium proportions resulting into different $V_{1/2}$ and C_{max}, see Table II. The simulated conversion losses of the both varactors are presented in Fig. 4.

As the ferroelectric varactors are known to have strong temperature dependence, the temperature dependence of the conversion loss was simulated. It turned out that the varactor with the lower conversion loss operates at only very narrow temperature range of approximately 10°C.

TABLE II. THE PARAMETERS OF SIMULATED FERROELECTRIC VARACTORS.

	Varactor 1	Varactor 2
Capacitor area	$A = 1\,\mu\text{m}^2$	
Film thickness	$d = 100$ nm	
Parasitic resistance	$R_p = 500\,\Omega$	
Parasitic capacitance	$C_p = 20$ fF	
Temperature	$T = 290$ K	
Proportion of barium	$x = 0.25$	$x = 0.6$
Half capacitance voltage	$V_{1/2} = 2$ V	$V_{1/2} = 60$ mV
Zero field capacitance	$C_{max} = 57.0$ fF	$C_{max} = 587.8$ fF

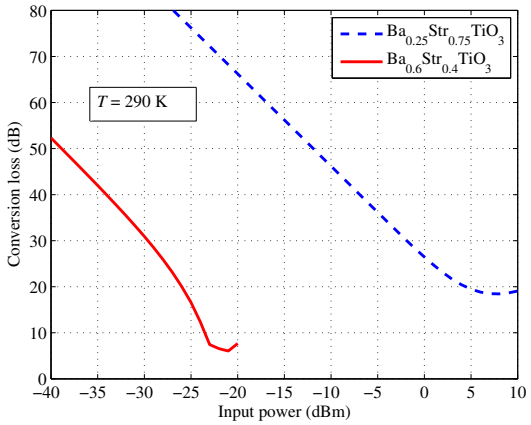

Figure 4. The simulated conversion losses of ferroelectric varactors.

C. *MEMS Resonator as a Mixing Element*

In radio engineering, the microelectromechanical systems (MEMS) technology has been widely used for example in phase-shifters, switches, varactors, filters and antennas. MEMS-based mixer-filter is also proposed for simultaneous mixing and filtering of radio frequency signal [16].

Electrostatically actuated MEMS resonators mix signals through different mechanism than diodes or ferroelectric varactors [17]. The electrical force affecting to MEMS cantilever is proportional to the squared voltage. Therefore, when two sinusoids at frequencies f_1 and f_2 are applied into a MEMS resonator, the resonator is actuated at frequencies 0, f_1, f_2, $2f_1$, $2f_2$, f_1+f_2 and f_1-f_2. If the mechanical resonance occurs at f_1-f_2, the resonator begins to oscillate at that frequency. Due to the oscillating capacitance, MEMS resonator modulates the reflected signals and one reflection occurs at $2f_1-f_2$.

The simulated conversion losses of different MEMS resonators (presented in Table III) are shown in Fig. 5.

MEMS resonators offers very low conversion loss, but their drawback is narrow bandwidth. For example, the bandwidth of resonator with Q_m=1000 is only 100 Hz. Due to this very narrowband operation, the radar is not capable to detect the range of the reflector but only its direction.

TABLE III. THE PARAMETERS OF SIMULATED MEMS RESONATORS.

Quality factor	$Q_m = 1, 10, 100, 1000$
Mass	$m = 108\,\mu$g
Capacitance	$C_0 = 354$ fF
Gap height	$g_0 = 100$ nm
Natural frequency	$f_0 = 100$ kHz

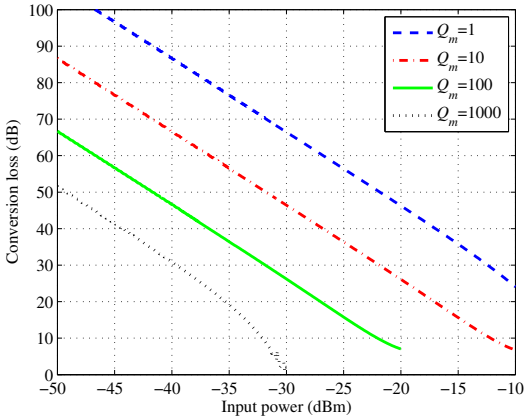

Figure 5. The simulated conversion losses of MEMS resonators.

D. *Wearable Antennas*

The body-worn tags should preferably be integrated in jackets and coats. For durability and comfort to the user, they should be built on thin flexible substrates. There are different flex films providing sufficient etching accuracy for W-band antenna. Rogers liquid crystal polymer (LCP) Ultralam 3000 [18], [19] with 100 μm thickness is one example, with good mechanical properties, low cost, and excellent electrical properties at high frequencies. Particularly, the moisture absorption of LCP is extremely low compared to other polymer based materials. Furthermore, antennas on LCP can be fabricated in a roll-to-roll process enabling low manufacturing costs. Taconic HyRelex TF-260 [20] with 76 μm thickness is another possibility. An array antenna including feed network can be realized with a single metal layer, without metal vias. The back of the flex film is fully metallised to form a ground plane for the antenna and circuits, and also to prevent body proximity affecting antenna performance.

Single, double, and four column microstrip patch array antennas are designed and characterized. Table IV shows the measured data on the antenna gain and half power beam width (HPBW) in elevation and azimuth, respectively. According to the system requirements, a tag antenna needs to achieve a gain of more than 15 dBi, and a vertical beamwidth of greater than 20°. The horizontal beamwidth should be as large as possible if the gain requirement can be fulfilled. Based on the experimental results shown in Table IV, the presented four column array antenna is regarded as an appropriate candidate for the proposed application.

The schematic layout of the antenna is shown in Fig. 6 and its measured radiation pattern cuts in Fig. 7. Its bandwidth is found to be 2.5 GHz, covering the 76–77 GHz band with a good margin.

TABLE IV. MEASURED ANTENNA GAIN AND HALF POWER BEAM WIDTH (HPBW).

	Gain (dBi)	HPBW in elevation (°)	HPBW in azimuth (°)
Single-column array	11.4	23	70
Double-column array	14.0	21	32
Four-column array	16.4	21	16

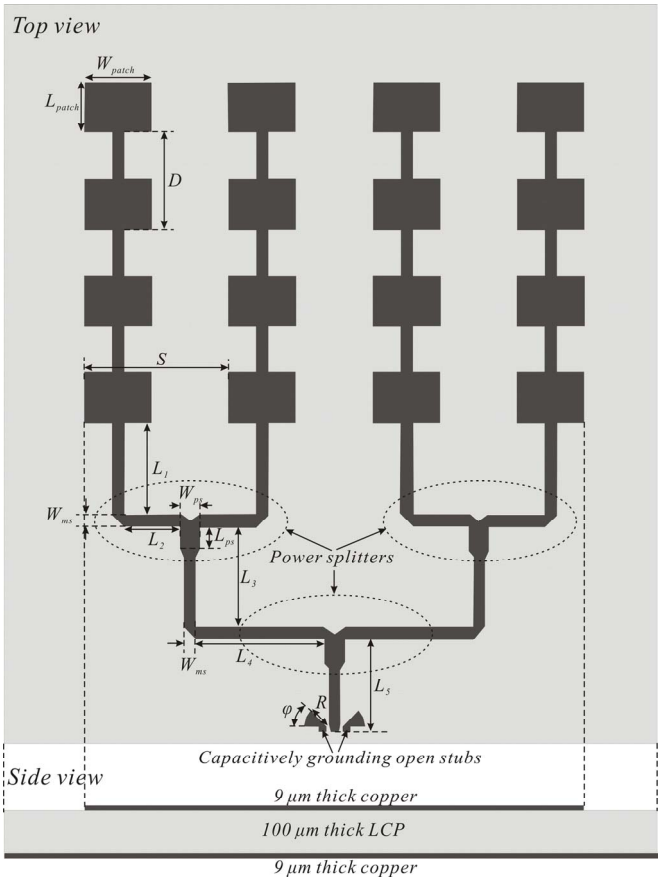

Figure 6. Schematic of the four column patch array antenna. Dimensions are: L_{patch}=1.04 mm, W_{patch}=1.40 mm, D=2.00 mm, S=3.00 mm, L_1=2.00 mm, L_2=1.119 mm, L_3=2.18 mm, L_4=2.69 mm, L_5=1.81 mm, L_{ps}=480 μm, W_{ps}=395 μm, W_{ms}=234 μm, R=0.46 mm, and φ=45°.

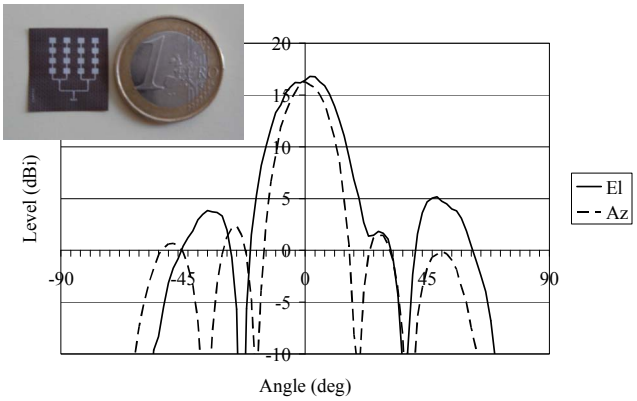

Figure 7. Measured elevation and azimuth cuts of the radiation pattern of fixed-beam high-gain tag antenna.

Directive tag antennas such as this necessitate several tags around the body for full coverage in azimuth. With the proposed antenna design, the cost per tag is estimated to be a few cents, making it feasible to integrate tens of tags in a jacket or coat. With a peak antenna gain of 16.4 dBi, at least 15 dBi will be achieved at some tag, at all azimuth angles.

IV. Estimated Detection Range

Let us estimate the achievable detection range with different mixing elements. According to the Friis transmission equation, the power received by the tag is

$$P_{r,tag} = P_t G_{radar} G_{tag} \left(\frac{\lambda}{4\pi r} \right)^2, \quad (2)$$

where P_t is the transmitted power, G_{radar} is the radar antenna gain, G_{tag} is the tag antenna gain, λ is the wavelength and r is the range. The backscattered power received by the radar is

$$P_{r,radar} = \frac{P_{t,radar} G_{radar}^2 G_{tag}^2}{L} \left(\frac{\lambda}{4\pi r} \right)^4, \quad (3)$$

where L is the conversion (mixing) loss of the tag. The sensitivity of the receiver is limited by the noise temperature of the radar receiver. Assuming 270 K antenna temperature, 7 dB noise figure of the receiver and 200 kHz noise bandwidth, the equivalent noise power of the receiver is –114 dBm. The realised tag antenna gain is 15 dBi and the estimated gain of the radar antenna is 40 dBi (equals to 0.01 m^2 aperture size). Using these parameters listed in Table V, the estimated detection ranges are 22 m with the Schottky diode, 39 m with the ferroelectric varactor and 74 m with the MEMS resonator.

TABLE V. The Estimated Parameters Used for Link Budget Calculations.

Transmitted power	$P_t = 16$ dBm
Gain of the radar antenna	$G_{radar} = 40$ dBi
Gain of the tag antenna	$G_{tag} = 15$ dBi
Wavelength	$\lambda = 3.9$ mm ($f = 77$ GHz)
Antenna temperature	$T_A = 270$ K
Receiver noise figure	$NF = 7$ dB
Noise bandwidth	$B = 200$ kHz
Noise power	$P_n = -114$ dBm

V. Conclusions

In this paper we have proposed automotive intermodulation radar for detecting and identifying VRUs equipped with nonlinear radar reflectors. We have presented possible solutions to the different building blocks of the intermodulation radar and described possible radar architecture. Radar reflector antenna structures that enable wearable radar reflectors (can be integrated into clothes) are studied and the first prototype antenna is characterized. Different mixing elements of the radar reflector are studied by simulations and the corresponding detection ranges are estimated. The MEMS resonator offers the longest detection range and the Schottky diode the shortest. However, very narrow bandwidth of the MEMS resonator does not allow detecting the range but only the direction. High temperature sensitivity of the ferroelectric varactor limits its operational temperature range.

References

[1] Annual Statistical Report 2007, SafetyNet project report, Deliverable D 1.16, February 2008, 64 p.

[2] V. Viikari, T. Varpula, and M. Kantanen, "Automotive radar technology for detecting road conditions. Backscattering properties of dry, wet, and icy asphalt," *Proceedings of the 5th European Radar Conference* Amsterdam, The Netherlands, Oct. 30 – 31, 2008, pp. 276 – 279.

[3] H. Staras and J. Shefer, Harmonic Radar Detecting and Ranging System for Automotive Vehicles, US Patent 3781879, 1972.

[4] E. T. Cant, A. D. Smith, D.R. Reynold and J. L. Osborne, "Tracing butterfly flight paths across the landscape with harmonic radar," *Proceedings of the Royal Society B: Biological Sciences*, Vol. 272, No. 1565, pp. 785 – 790, Apr. 2005.

[5] J. R. Riley and A. D. Smith, "Design considerations for an harmonic radar to investigate the flight of insects at low altitude," *Computers and Electronics in Agriculture*. Amsterdam, The Netherlands: Elsevier, 2002, Vol. 35, pp. 151 – 169.

[6] B. G. Colpitts and G. Boiteau, "Harmonic radar transceiver design: Miniature tags for insect tracking," *IEEE Transactions on Antennas and Propagation*, Vol. 52, No. 11, pp. 2825 – 2832, Nov. 2004.

[7] Standard, ETSI TR 101 982 V1.2.1, July 2002.

[8] Standard, ETSI EN 301 091-1 V1.3.3, Nov. 2006.

[9] Standard, ETSI TR 102 263 V1.1.2, Feb. 2004.

[10] H. Rohling and M.-M. Meinecke, "Waveform Design Principles for Automotive Radar Systems," *Proceedings of the CIE International Conference on Radars*, 2001, pp. 1-4.

[11] A. V. Räisänen, "Frequency multipliers for millimetre and submillimeter wavelengths," *Proceedings of the IEEE*, Vol. 80, No. 11, pp.1842 – 1852, Nov. 1992.

[12] V. Möttönen, "Receiver front-end circuits and components for millimetre and submillimetre wavelengths," D.Sc. dissertation, Dept. of Electrical and Communications Engineering, Helsinki University of Technology, Espoo, Finland, 2005.

[13] A. K. Tagantsev, V. O. Sherman, K. F. Astafiev, J. Venkatesh, and N. Setter, "Ferroelectric materials for microwave tunable applications," *Journal of Electroceramics*, No. 11, pp. 5 – 66, 2003.

[14] O. G. Vendik, E. K. Hollmann, A. B. Kozyrev, and A. M. Prudan, "Ferroelectric tuning of planar and bulk microwave devices," *Journal of Superconductivity*, Vol. 12, No. 2, pp. 325 – 338, 1999.

[15] D. R. Chase, L-Y. Chen, and R. A. York, "Modelling the capacitive nonlinearity in thin-film BST varactors," *IEEE Trans. on Microwave Theory and Techniques*, Vol. 53, No. 10, pp. 3215 – 3220, Oct.2005.

[16] A.-C. Wong and C. T.-C. Nguyen, "Micromechanical mixer-filters ("mixlers")," *IEEE Journal of Micromechanical Systems*, Vol. 13, No. 1, pp. 100 – 112, Feb. 2004.

[17] H. Seppä, "Method and apparatus for converting electromagnetic energy of objects," European Patent EP1183550A1, June 2002.

[18] www.rogerscorporation.com, Rogers Corporation, Ultralam 3000 Data Sheet.

[19] S. L. Smith and V. Dyadyuk, "Measurement of the dielectric properties of Rogers R/flex 3850 liquid crystalline polymer substrate in V and W band," *Proceedings of the International Symposium of IEEE Antennas ad Propagation Society*, Vol. 4B, July 2005, pp. 435-438.

[20] www.taconic-add.com.